Supplementary figures & figure legends

Supplemental Figure S1

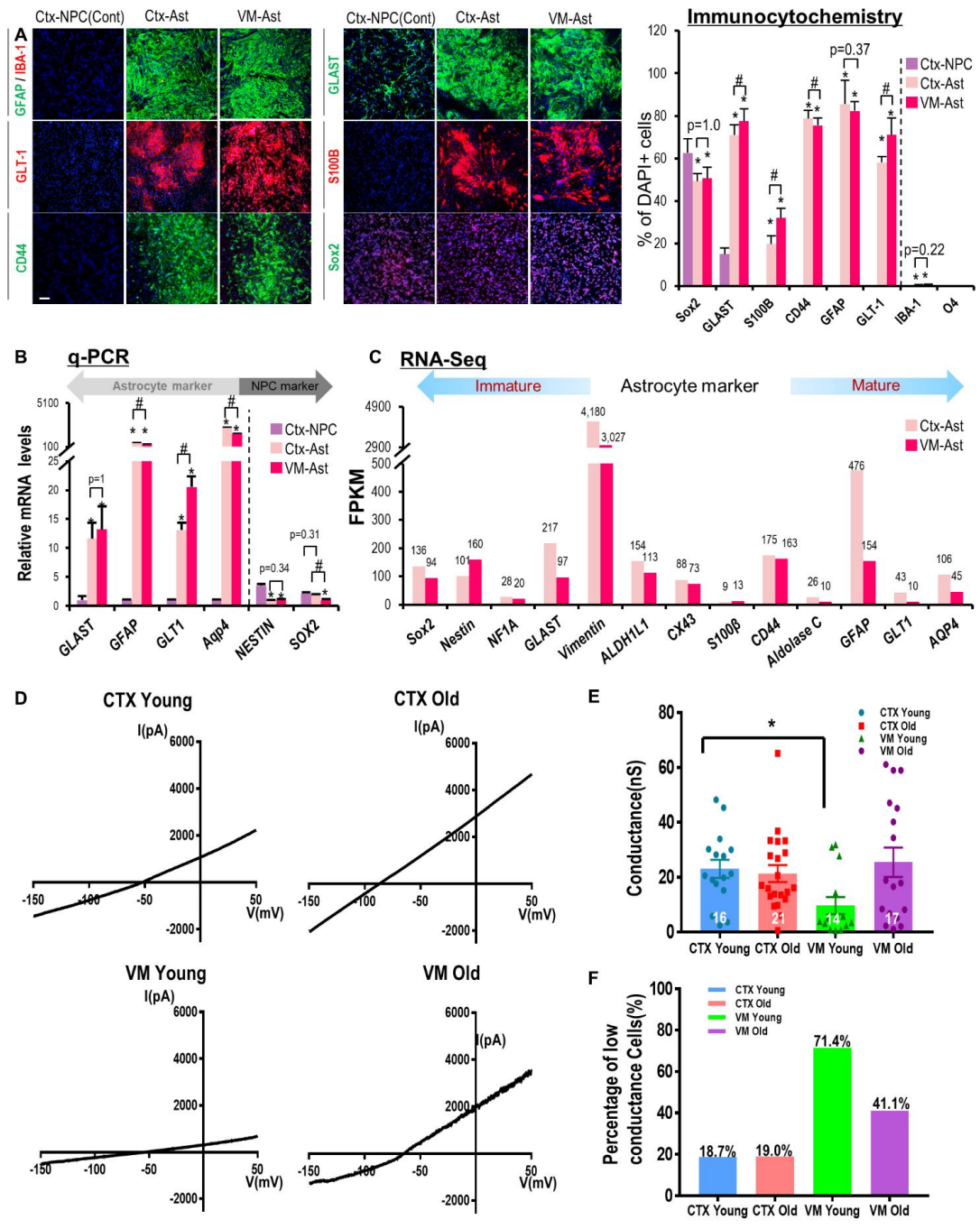

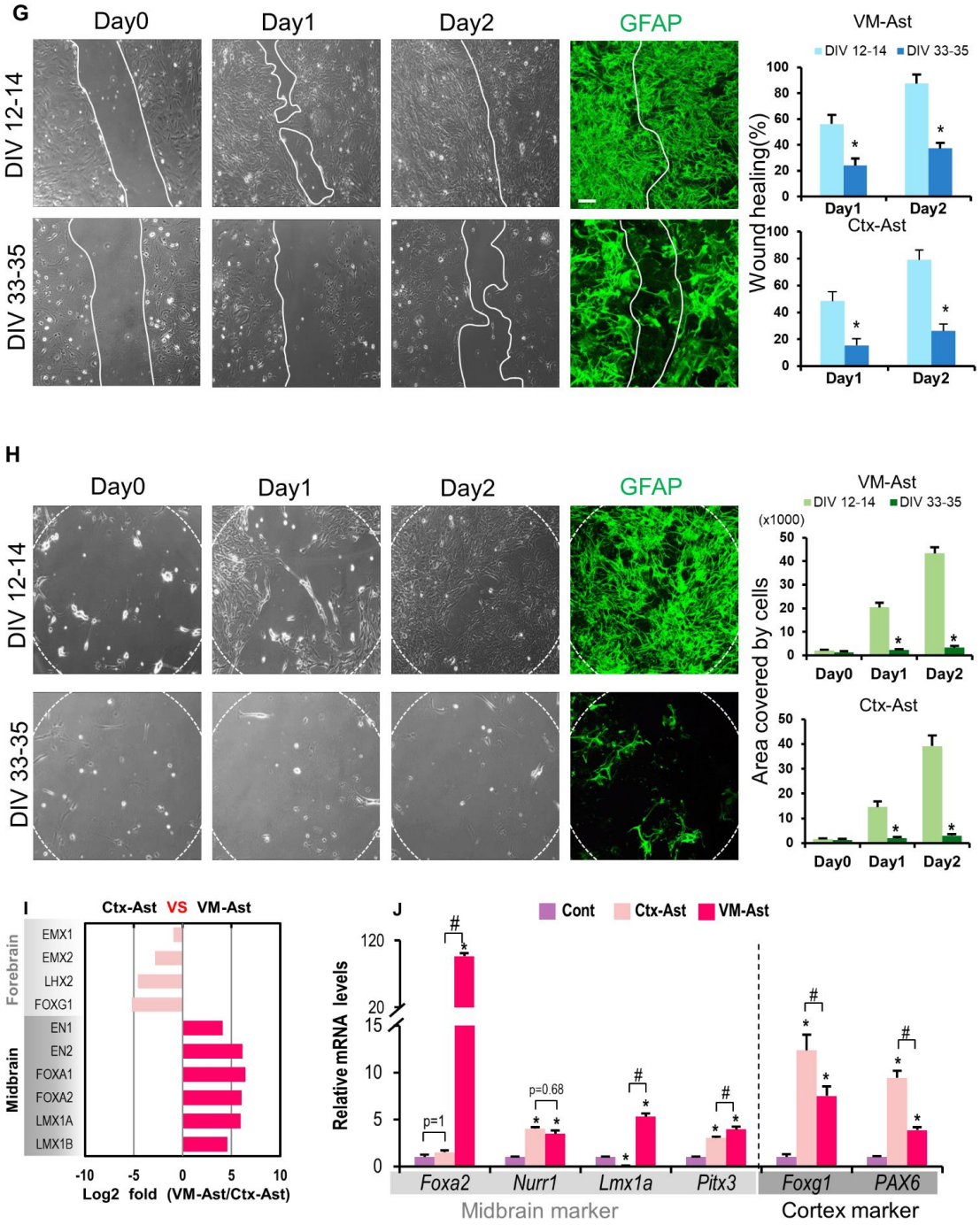

Suppl. Fig. S1. Immature and brain region-specific identities of the astrocytes cultured from mouse cortices and VM. A and B, Expression of astrocytic markers estimated by immunocytochemical(A) and real-time qPCR(B) analyses. Undifferentiated NPCs derived

from mouse embryonic cortices (Ctx-NPC) were used as the control. Data present mean±SEM of four(A) and three(B) experiments. Scale bar, 50 um. C, Gene expression levels of immature and mature astrocytic markers in the cultured astrocytes, estimated by FPKM in the RNA-seq data. The FPKM value is shown above each bar in the graph. D-F, Patch-clamp electrophysiological analysis on cultured astrocytes derived from cortex and VM at DIV 14 and 35. Shown in (D) are representative traces for the voltage ramp-induced whole-cell passive conductance currents recorded from each cell. E, Summary bar graph of average conductance. Number of cells analyzed is indicated in each bar. P-values were obtained with one-way ANOVA (Kruskal-Wallis test). *P<0.05. F, Percentage of the number of cells showing low conductance (<10nS) from each group. G-H, Regenerative capacity of cultured astrocytes associated with astrocyte maturity were assessed after scratch injury (G) and in an inhibitory proteoglycan environment (H). Scratch injury (G) and aggrecan/laminin gradient spots (H) were generated on cultured Ctx- and VM-astrocytes at DIV12-14 and 33-35 as described in the Materials and Methods. % areas filled by astrocytic cells between the two edges of the scratch (G) and numbers of cells that grew inward the spots (H) were measured during 2 days. Shown are the representative phase-contrast and GFAP-immunofluorescent images of VM astrocytes at DIV12-14 and 33-35. *p<0.01, n=6, Student t-test. Scale bars, 100μm. I and J, Region-specific gene expression in the cultured Ctx- and VM-astrocytes was assessed by RNA-seq (I) and qPCR (J) analyses. Significantly different from the Ctx-NPC control* and Ctx-astrocytes# at p<0.05, n=3 PCR reactions, ANOVA.

Supplemental Figure S2

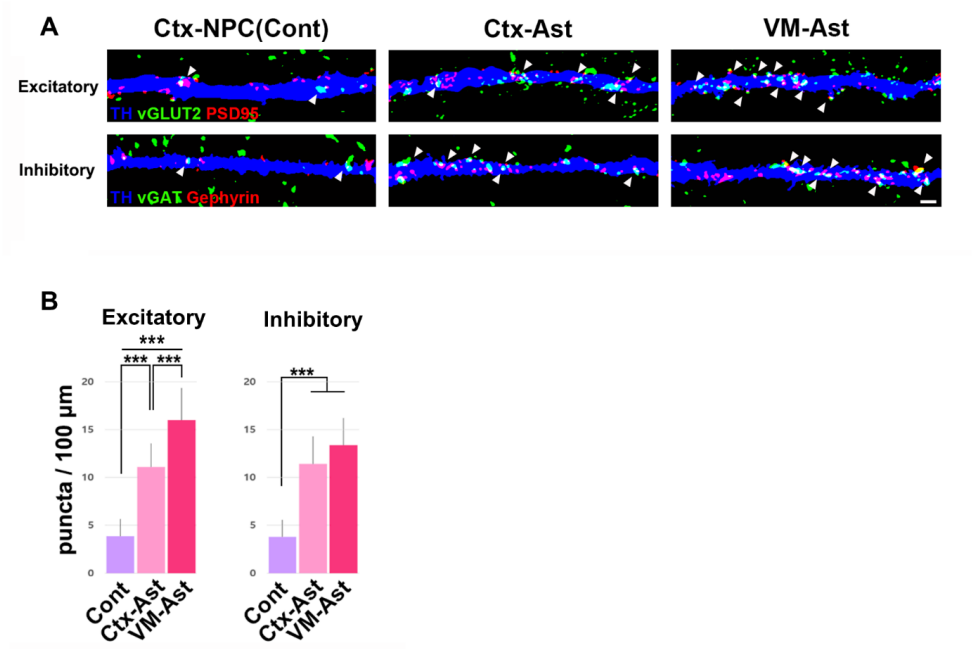

Suppl. Fig. S2. Glutamatergic excitatory and GABAergic inhibitory synaptic formation. A, Immunocytochemistry of dendrites in TH+ fibers of cultured mDA neurons colabeled with antibodies against glutamatergic presynaptic marker vesicular glutamate transporter 2 (vGlut2) and the excitatory post-synaptic marker post-synaptic density protein 95 (PSD95) or the GABAergic presynaptic marker vesicular GABA transporter (vGAT) and the inhibitory post-synaptic marker Gephyrin to visualize pre- and postsynaptic elements of excitatory or inhibitory synapses, respectively. Arrowheads point to vGlut2+/PSD95+ or vGAT+/ Gephyrin+clusters . B, Quantification of the synaptic puncta. Data represent mean ± SEM. ***$p < 0.01$ by ANOVA followed by Fisher's LSD post hoc test, n=8-16 for excitatory and 9-15 for inhibitory synapses. Scale bars, 2 µm.

Supplemental Figure S3

A

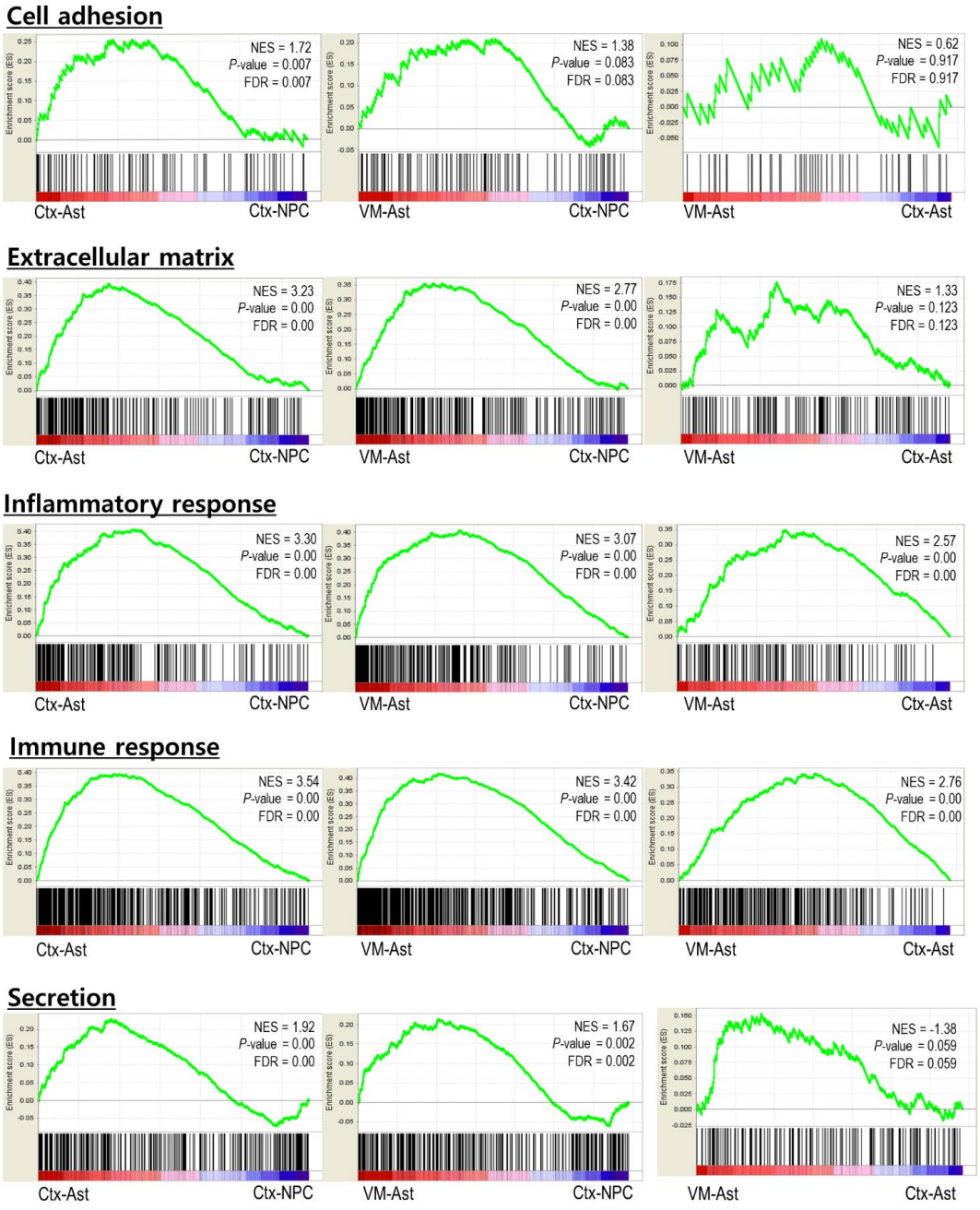

B

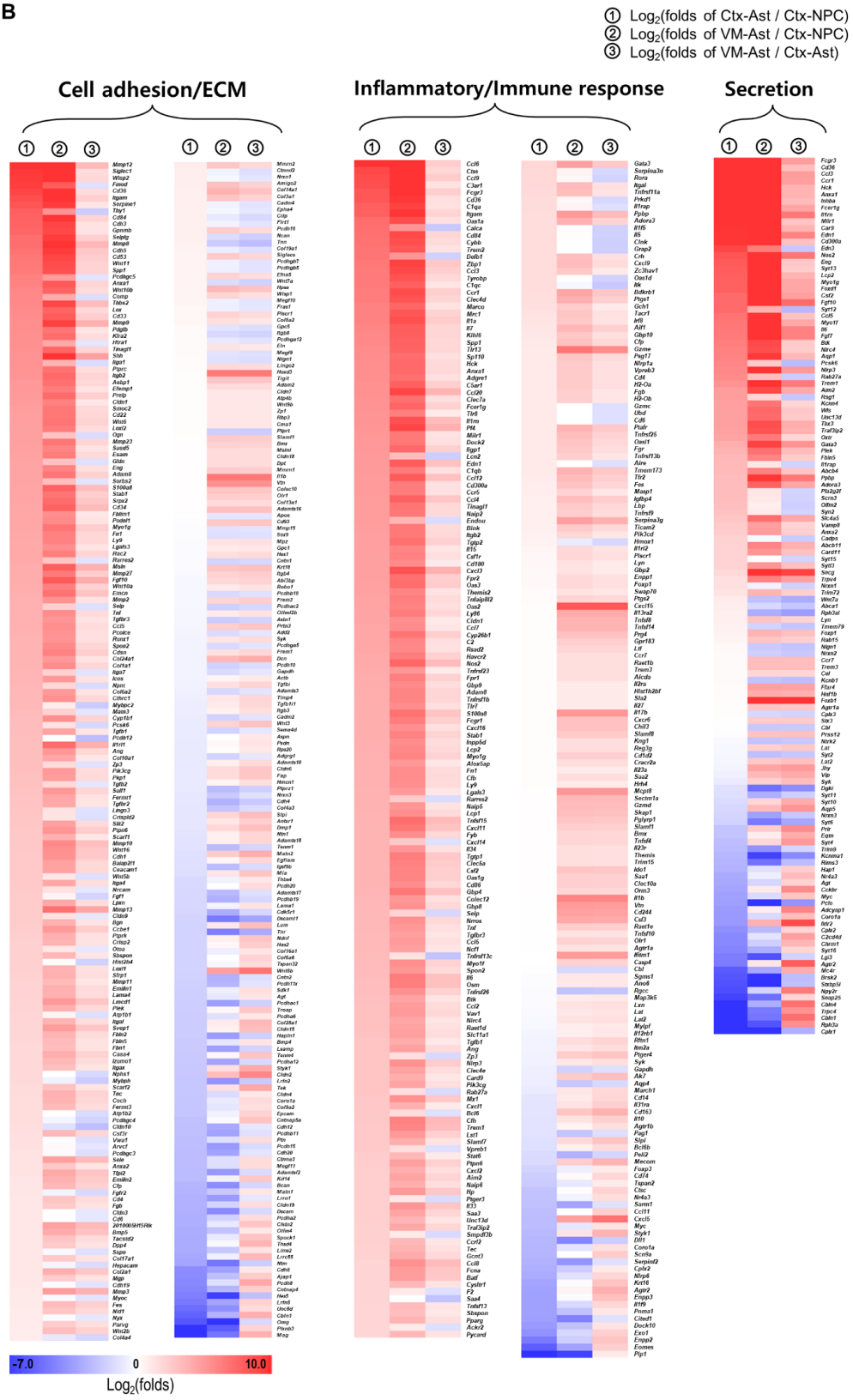
① Log2(folds of Ctx-Ast / Ctx-NPC)
② Log2(folds of VM-Ast / Ctx-NPC)
③ Log2(folds of VM-Ast / Ctx-Ast)
Cell adhesion/ECM
Inflammatory/Immune response
Secretion
-7.0
0
10.0
Log2(folds)

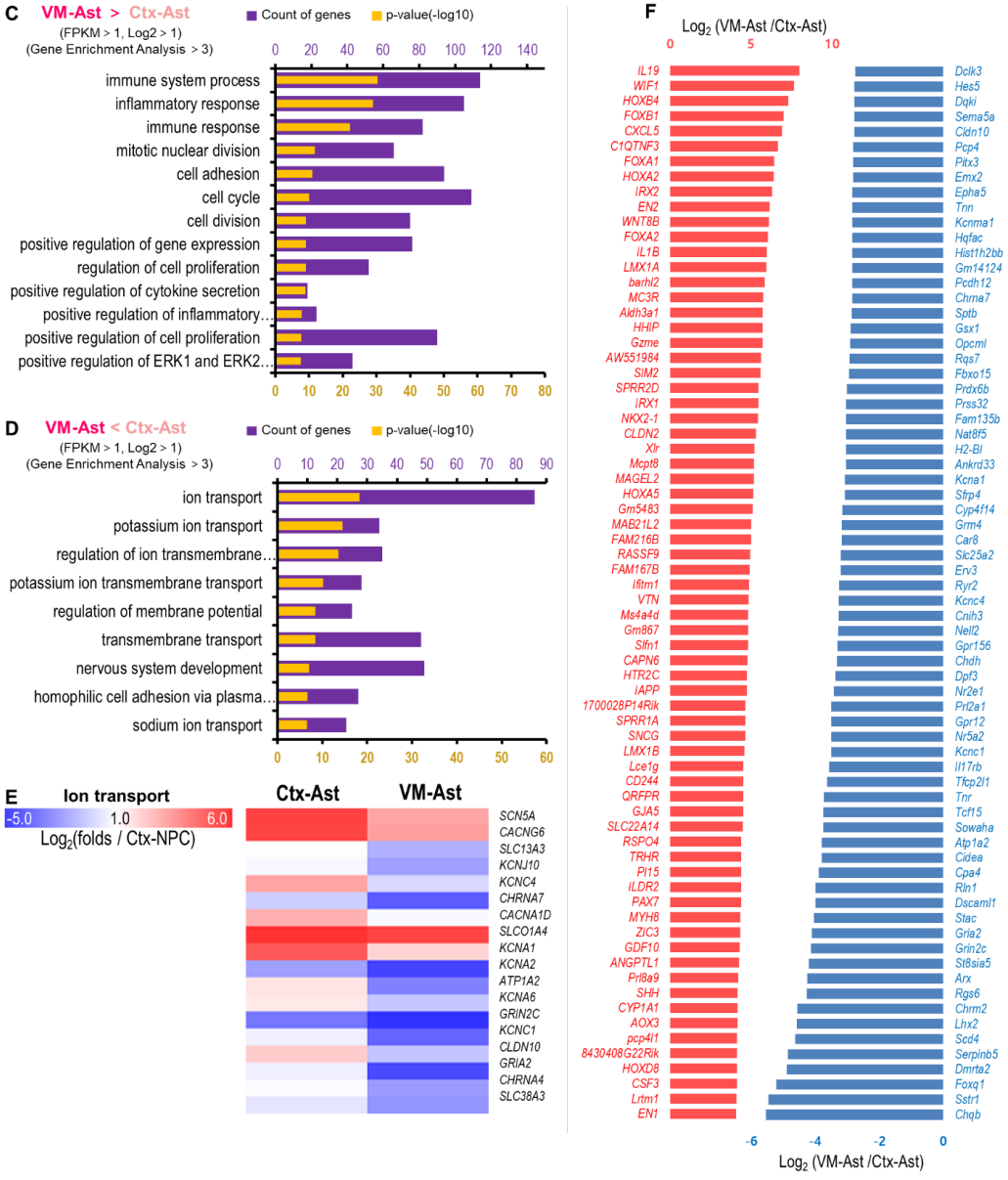

Suppl. Fig. S3. A, Gene set enrichment analyses (GSEA) for high-ranked GO and KEGG pathways in Fig. 4B and 4D. B, Heat-map for the gene expressions analyzed in A. Shown are Log2 fold changes of Ctx-astrocyte/Ctx-NPC①, VM-astrocyte/Ctx-NPC② and VM-astrocyte/Ctx-astrocyte③. C-D, GO analyses for the genes up-regulated (C) or down-regulated (D) in VM-astrocytes vs. Ctx-astrocytes (FPKM>1, log2>1). E, Heat-map for ion transporter genes, annotated to the 1st ranked ontology in the analysis for down-regulated

genes in VM-astrocytes vs. Ctx-astrocytes. F, The top 70 up-regulated and down-regulated genes in VM-astrocytes (vs. Ctx-astrocytes) are listed.

Supplemental Figure S4

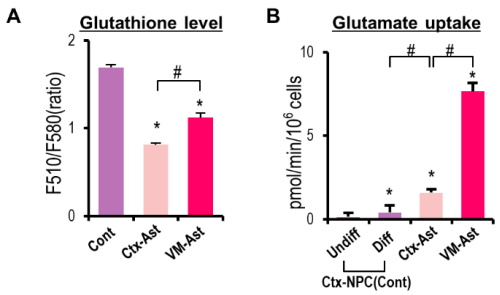

Suppl. Fig. S4. Neuroprotective activities of cultured astrocytes by eliminating oxidants and glutamate-mediated toxicity. A. Anti-oxidant capacity assessed by intracellular glutathione levels. B, Glutamate uptake activity. Undifferentiated and differentiated Ctx-NPCs (after 6 days of diff.) were used as the negative controls for glutamate uptake assays. *,#$p<0.05$, n= 4 (A), 3 (B), ANOVA.

Supplemental Figure S5

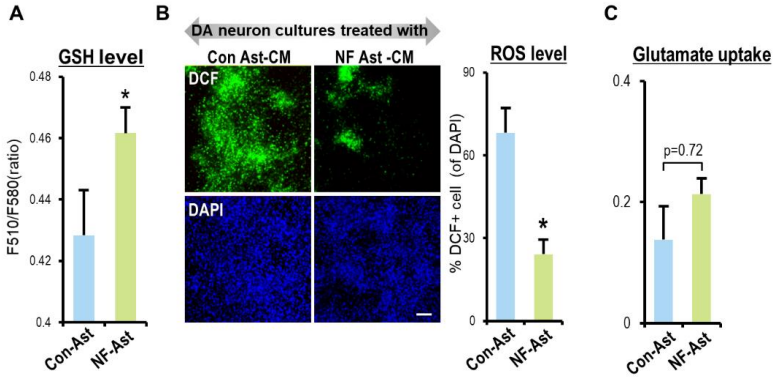

Suppl. Fig. S5. Effects of forced Nurr1+Foxa2 expression in VM-astrocyte-mediated ROS scavenging and glutamate clearance activities. A, Intracellular glutathione levels in control- vs. NF-astrocytes. B, ROS levels in mDA neuron cultures treated with NF-astrocyte CM or control-astrocyte CM. mDA neuron-enriched cultures were derived by differentiation of VM-NPCs and treated with CM prepared from N+F- or mock control-transduced VM-astrocytes. After cells were exposed to H_2O_2 (500 uM, 3 hrs), ROS levels, detected by DCF staining, were quantified by DCF+ cell counting. Scale bar, 100 um. C, Glutamate uptake activity. *$p<0.05$, n=3, Student's t-test (2-tailed).

Supplemental Figure S6

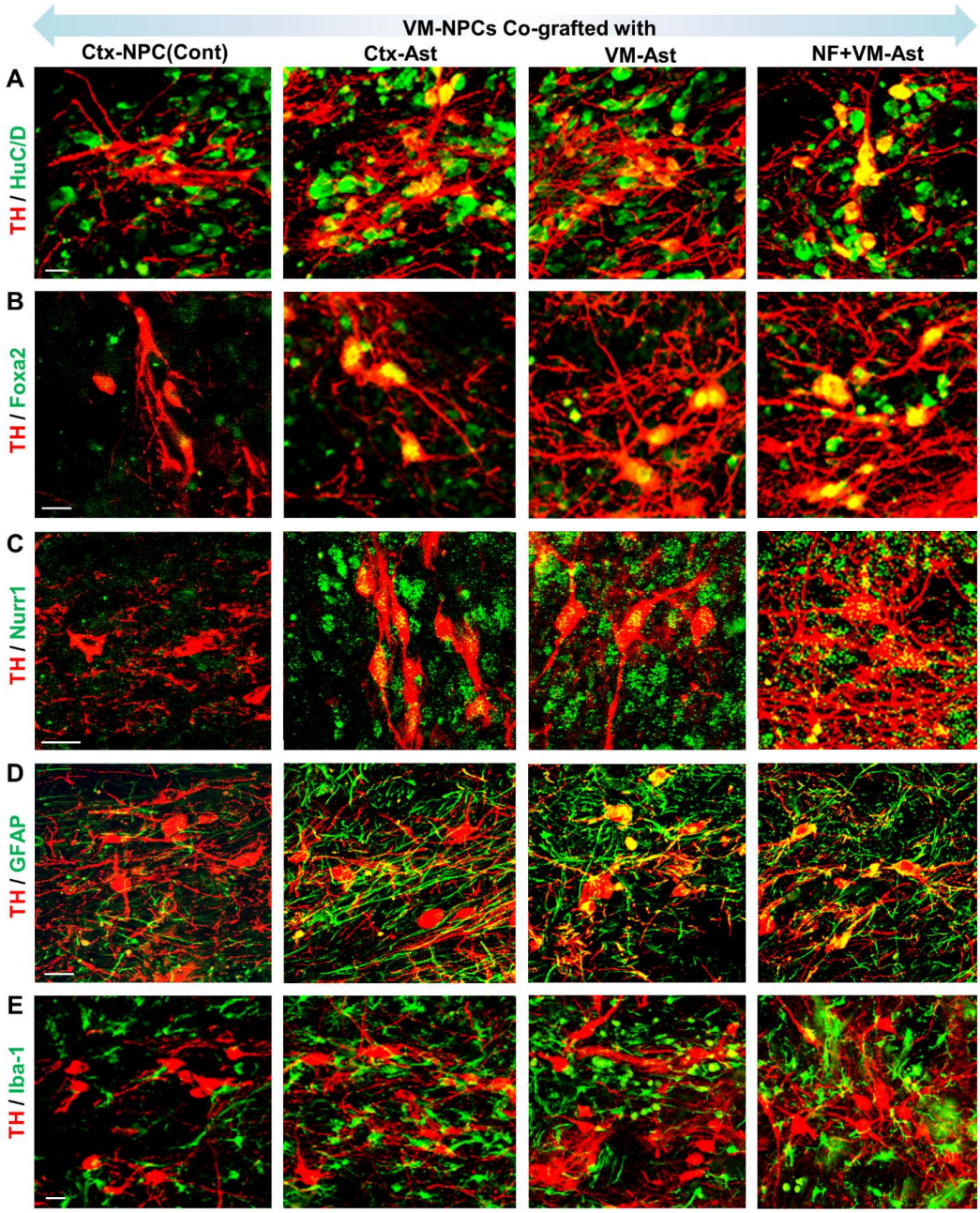

Suppl. Fig. S6. A-C, Co-expression of mature neuronal (HuC/D) and midbrain-specific mDA neuronal (Foxa2 and Nurr1) markers in TH+ DA cells at 6 months post-transplantation. D-E, Representative TH+/GFAP+ and TH+/Iba1+ cell images in the grafts. Scale bars, 25 um.

Supplemental Figure S7

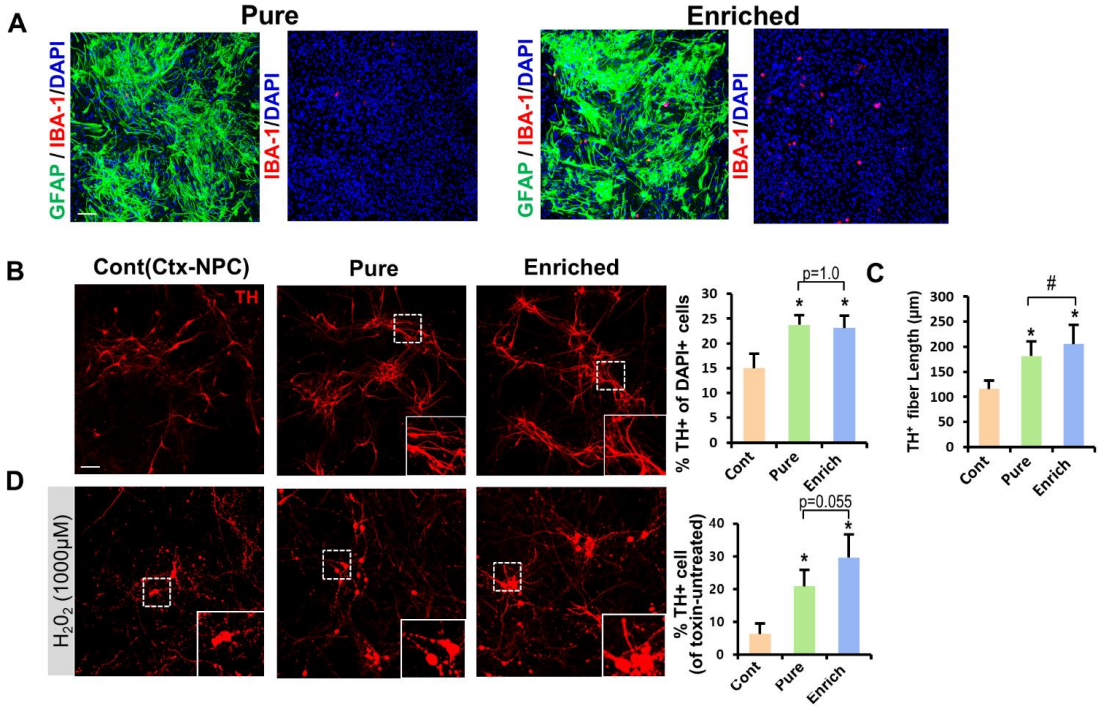

Suppl. Fig. S7. DA neurotrophic actions elicited by cultured VM-astrocytes in the absence or presence of minor microglia population. Pure (no Iba+ and O4+ cells) and enriched VM astrocyte cultures with minor microglia contamination (Iba+ cells: <0.5%) were prepared as described in the Materials and Methods. A, Representative images for GFAP+/Iba1+/DAPI+ (left) and Iba+/DAPI+ (right) cells. B-D, E12 VM-NPCs during differentiation were treated with the CM prepared from the astrocyte cultures. mDA neuron differentiation, morphologic maturation, and resistance to toxic insult were assessed by TH+ mDA neuron yields at D6 (B), TH+ neurite lengths at D12 (C), and viable TH+ cells survived after H2O2 treatment (1000 uM, 8 hrs) at D12(D), respectively. *,#p<0.05, n= 6, Scale bar, 50 μm.

Supplemental Figure S8

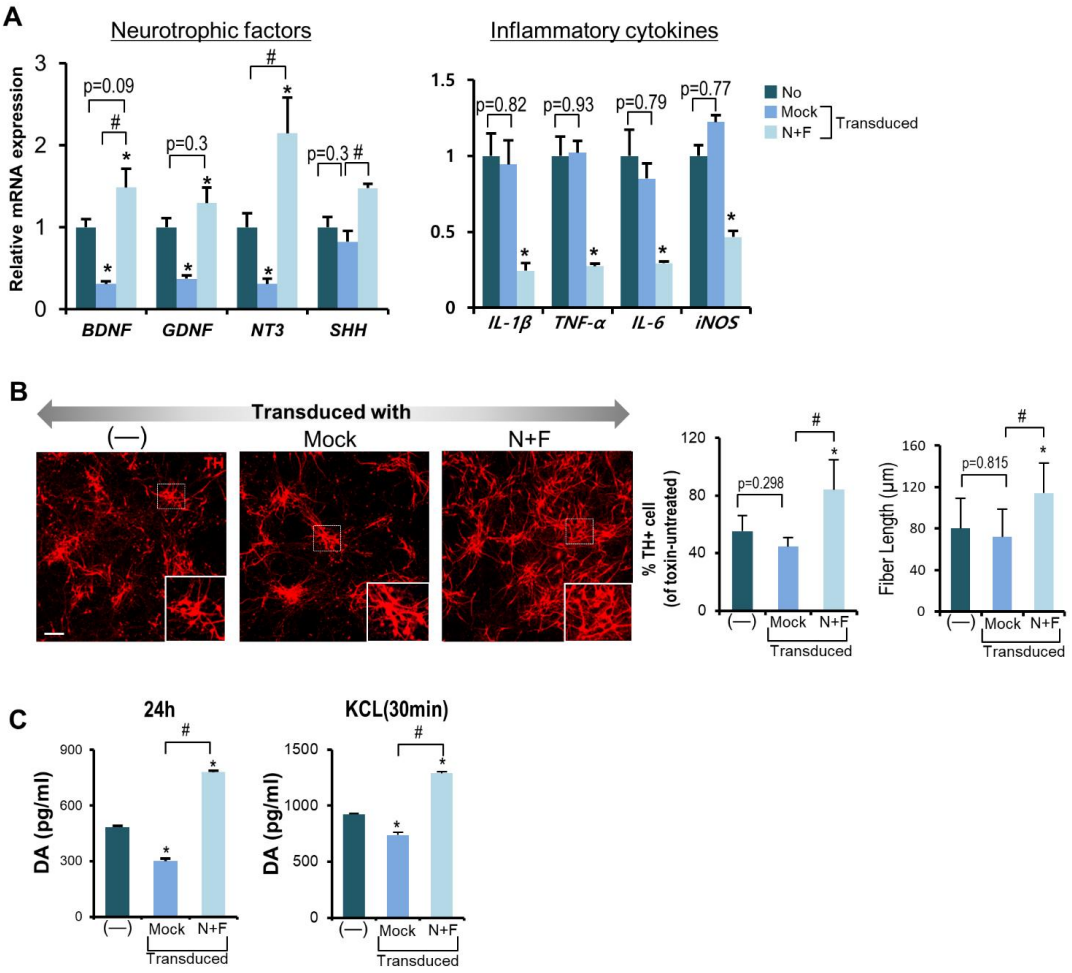

Suppl. Fig. S8. Effects of viral transduction on astrocyte-mediated neurotrophic actions. VM-astrocytes (non-transduced), those transduced with mock control and with Nurr1+Foxa2-expressing lentiviruses were subjected to qPCR analyses to assess expressions of neurotrophic factors and pro-inflammatory cytokines (A). CMs were prepared from the non-transduced and transduced VM-astrocytes. In the presence of the CM supplementation, cell viability against H2O2 toxin (B) and pre-synaptic DA release (C) were assessed in the cultures differentiated from VM-NPCs at differentiation day 12. Significantly different from the non-transduced* and mock-transduced# controls at $p<0.05$, ANOVA, n= 4. Scale bar, 50 μm.

Supplemental Figure S9

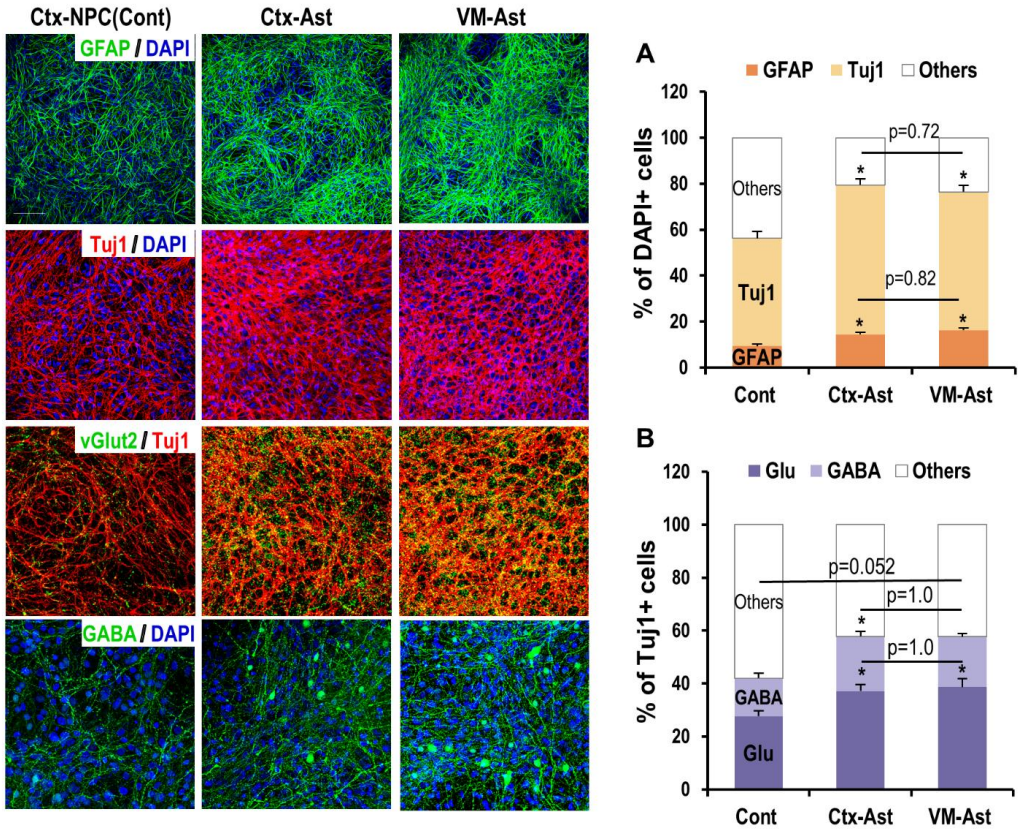

Suppl. Fig. S9. Pan-trophic actions of cultured astrocytes. VM-NPCs were differentiated in the absence or presence of CM prepared in cultured Ctx- or VM-astrocytes. Yields of total TuJ1+ neurons and GFAP+ astrocytes (A) and glutamatergic (vGlut2+/TuJ1+) and GABAergic (GABA+) neuronal subtypes (B) were assessed. *Significantly different from the untreated control at $p<0.05$, ANOVA, n= 4. Scale bar, 50 μm.

Supplementary Methods

Astrocyte functional assays

Electrophysiological recording in cultured astrocytes

Cultured astrocytes were plated onto coverslips and maintained in DMEM supplemented with 10% fetal bovine serum and 10% horse serum for at least 24 h before electrophysiology experiments. For electrophysiological recording, the patch pipettes had an open-tip resistance of 4-7MΩ when filled with a pipette solution containing (in mM): 150 KCl, 1 CaCl2, 1 MgCl2, 5 EGTA and 10 HEPES (pH 7.2 was adjusted with KOH). Standard bath solution contained (in mM): 150 NaCl, 3 KCl, 2 CaCl2, 1 MgCl2, 10 HEPES, 5.5 D-glucose and 20 sucrose (pH 7.4was adjusted with NaOH). The mean membrane resistance of hippocampal astrocytes in culture was 7.45±0.76 mega ohms (mean±s.e.m.), and the series resistance was <30 mΩ, which we monitored throughout all experiments. Recording pipettes were fabricated from borosilicate glass capillaries (World Precision Instruments) using a P-97 Flaming/Brown micropipette puller (Sutter Instruments).Whole-cell membrane currents were amplified by the Axopatch 200A. Currents were elicited by 1-s ramps from -150mV to +50mV (from a holding potential of -70 mV). Data acquisition was controlled by signals between amplifier and computer. Data were sampled at 5 kHz and filtered at 2 kHz. Cell membrane capacitance was measured by using the membrane test protocol built into pClamp10.0. The calculated and measured junction potentials were -2.6mV and -2.5 mV, respectively.

Scratch injury assay

Using a sterile pipette tip, scratches were made on the monoconfluent cell layer of astrocytes. The plates were then rinsed with sterile PBS to remove cell debris and replaced with fresh cell culture media. At 0, 1 and 2 days after scratch, the area occupied by astrocytes were measured between the two edges of the scratch using Image J software.

Growing capacity in inhibitory proteoglycan environment

Gradient spot glass coverslips (12 mm) were prepared as described previously (1). Briefly,

coverslips coated with poly-L-lysine (PLL; Sigma-Aldrich, St. Louis, MO) and nitrocellulose were spotted with 2 ul of a solution of aggrecan (0.7 mg/mL; Sigma-Aldrich) and laminin (5 ug/ mL; Biomedical Technologies, Stoughton, MA) in Ca++, Mg++-free Hank's Balanced Salt Solution (CMF; Invitrogen, Gaithersburg, MD). The spots were allowed to dry and were then covered with laminin (5 ug/ mL) in CMF and kept at 37℃ until just before cell plating (for 3 h). The laminin solution was removed before plating astrocytes ($2x10^4$ cells/well in 24-well plate). Migratory potentials of astrocytes inward the gradient aggrecan/laminin spots were determined by the areas covered by astrocytes in the spots during 2 days.

Morphometric assessments

To estimate morphological maturation, total fiber length and soma size (perimeter) of randomly selected TH+ DA neurons were measured using an image analysis system (Leica LAS). TH+ DA neuron images were also reconstructed using Neurolucida 360 (MicroBrightfield, Inc.). Complexity of the fibers in TH+ cells was further assessed using the Sholl test. The number of intersections of the neurite tree with increasing perimeters from the center of the soma was counted every 15 μm up to a distance of 200 μm. The critical value of the radius at which there is a maximum number of neurites was also determined in the Sholl test. Neurite length and branching of TH+ DA neurons were further assessed using time-lapse imaging as described below.

Time-lapse imaging of neuron axonal elongation

VM-NPCs from the mouse embryos at E10.5 were seeded at 4.0×10^4 cells in each well of a 24-well plate and cultured. CMs were treated from 3 days after differentiation and diluted with N2 medium (1:1, v:v) to induce neurite elongation. Phase contrast microscopic images were automatically taken using the IncuCyte ZOOM Live Cell Imaging System (Essen Bioscience, Ann Arbor, MI, USA) every 2 h for 42 hours. Neurite lengths and branch points of the neurites were automatically analyzed with IncuCyte's NeuroTrack software.

Messenger RNA expression analysis

Total RNA was prepared using the Trizol Reagent (Invitrogen, Carlsbad, CA, USA) through the RNA isolation protocol. cDNA synthesis was carried out using a Superscript kit

(Invitrogen). Real-time PCR was performed on a CFX96™ Real-Time System using iQ™ SYBR green supermix (Bio-Rad, Hercules, CA, USA) and gene expression levels were determined relative to GAPDH levels. The Mouse Oxidative Stress RT² Profiler™ PCR Array (cat. 330231 PAMM-065ZA) was used to profile the expression of 84 genes related to oxidative stress using a RT^2 Profiler PCR Array^R (Qiagen, Gaithersburg, MD, USA). Primer information is shown in Supplementary Table 1.

RNA-seq analysis

RNA sequencing was carried out in Macrogen (Seoul, Korea). After trimming reads with a quality score less than 20 using FastQC and checking the mismatch ratio using Bowtie, all RNA-seq data were mapped to the mouse reference genome (GRCm38/mm10) using STAR (2). To measure expression levels of all 46,432 annotated genes, 107,631 transcripts, and 76,131 protein-coding (mRNA) records in the mouse genome (based on NCBI RefSeq annotations Release 105: February 2015), we counted reads mapped to the exons of genes using Htseq-count and calculated the Fragments Per Kilobase of exon per Million fragments mapped (FPKM) value. Quantile normalization was performed to reduce technical global bias of expression between groups (3).All data have been deposited into GEO database (GEO: GSE106216).

Determination of intracellular ROS and glutathione levels

For measurement of intracellular ROS levels, cells were incubated with 10 μM of 5-(and-6)-chloromethyl-2′,7′-dichlorodihydro-fluorescein diacetate [CM-H_2DCF-DA (herein referred to as DCF) (Invitrogen)] for 10 min. The cells were then washed with D-PBS (in mM: 2.68 KCl, 1.47 KH_2PO_4, 136.89 NaCl, and 8.1 Na_2HPO_4), and fluorescence and phase-contrast images were taken using an Olympus microscope (IX71, Hicksville, NY, USA). Determination of intracellular glutathione levels was requested and carried out by Cell2in (www.cell2in.com, Seoul, Korea).

DA release assay

The pre-synaptic activity of DA neurons was determined by measuring the levels of DA neurotransmitter released in the differentiated VM-NPC cultures. Media incubated for 24 hrs

(differentiation day 12-13) was collected and used to determine the DA level using an ELISA kit (BA E-5300, LDN). In addition, DA release evoked by membrane depolarization was estimated by incubating the cultures (at differentiation day 12) in fresh N2 media in the presence or absence of 56 mM KCl for 30 min. The evoked DA release was calculated by subtracting the DA release without KCl from the DA level with KCl.

Glutamate uptake

Cells were washed twice in Tissue Buffer (5 mM Tris, 320 mM sucrose, pH 7.4) and exposed to 10 uM glutamate in either Na+-containing Krebs buffer (120 mM NaCl, 25 mM $NaHCO_3$, 5 mM KCl, 2 mM $CaCl_2$, 1 mM KH_2PO_4, 1 mM $MgSO_4$, and 10% glucose) or Na+-free Krebs (120 mM choline-Cl and 25 mM Tris-HCl) for 10 min at 37°C. Uptake was stopped by placing the cells on ice and washing them twice with Wash Buffer (5 mM Tris/160 mM NaCl, pH 7.4). Cells were collected and homogenized in 100 ul of assay buffer and the amount of glutamate in the cell homogenates was measured using a glutamate assay kit (Abcam, Cambridge, MA, USA , ab83389). Na+-dependent uptake was determined by subtracting Na+-free counts from total counts in the presence of Na+.

Brain clarity and 3D volume imaging

For 3D volume imaging of transplanted brain, we used Acrylamide-based tissue clearing protocol (REF: PMC4707495). Briefly, thick coronal brain slice (2-mm) containing transplanted cells in striaum was fixed in 4% PFA overnight at 4℃. Fixed sample was incubated in hydrogel monomer solution A4P0 (4% acylamide in 1X PBS) supplemented with 0.25% photoinitiator 2,2′-azobis[2-(2-imidazolin-2-yl)propane] dihydrochloride (Wako Pure Chemical, Osaka, Japan) overnight at 4℃ with gentle shaking. Hydrogel-infused sample was de-gassed for 2 min and polymerized for 2-3 hrs at 37℃. Polymerized sample was underwent electrophoretic tissue clearing (ETC) for 2 hrs using xClarity system (Logos Biosystems, Korea). Cleared sample was washed in 0.01X PBS at room temperature with gentle shaking, and was incubated in primary antibody dilution solution (TH, 1:500, in 0.1X PBS containing 6% BSA and 0.1% Triton X-100) for 2 days at 37℃. The stained sample was

washed with 0.1X PBS for 1 hr with gentle shaking and then stained with fluorescently conjugated secondary antibody for 2 days at 37℃. Stained sample was then washed with 0.1X PBS several times with gentle shaking, immersed in CUBIC-mount solution for 1 hr at room temperature. Fluorescence images were obtained on a conventional confocal microscope (Leica, TCS SP8) with either the HC PL APO 10X /0.40 CS (WD , 2.2 mm), HC FLUOTAR L 25X /0.95 W VISIR 0.17 (WD, 2.4 mm) objective lens. 3D reconstruction of the images and video were obtained from Z-stacks consisting of 136-358 optical slices, taken at intervals 2.4 to 0.5 ㎛ using Leica Application Suite X (LAS X) software.

Supplementary Table 1. Primer sequences used for qPCR reactions.

Gene	Primer Sequence(Sense/Antisense)	
AHR	GTC CTC AGC AGG AAC GAA AG	CCA GGG AAG TCC AAC TGT GT
AQP4	CGG TTC ATG GAA ACC TCA CT	CAT GCT GGC TCC GGT ATA AT
ARG1	TAT CGG AGC GCC TTT CTC TA	ACA GAC CGT GGG TTC TTC AC
BDNF	GTG ACA GTA TTA GCG AGT GGG	GGG TAG TTC GGC ATT GC
CCL17	AAT GTA GGC CGA GAG TGC TG	CAT GCT TGT CTT TGG GGT CT
CCL22	TTC TTG CTG TGG CAC TTC AG	CTT CTT CAC CCA GAG CAT CC
COL6A2	ATG GAC AGA AGG GCA AAC TG	CTT GCC TCC TTT CAC TCC TG
CXCL9	CTC ATG GGC ATC ATC TTC CT	TCA GCT TCT TCA CCC TTG CT
CXCL10	TCG TGC TGC TGA GTC TGA GT	GGC TCA CCG CTT TCA ATA AG
CXCL11	TAT GAT CAT CTG GGC CAC AA	CCA GGC ACC TTT GTC CTT TA
EPO	CCA GCC ACC AGA GAG TCT TC	TGC AGA AAG TAT CCG CTG TG
FGF8	TGT TGC ACT TGC TGG TTC TC	ACT CGG ACT CTG CTT CCA AA
FIZZ1	ATC TGC GTC TTC CTT CTC CA	CAG TAG CAG TCA TCC CAG CA
FN1	GAA AGG CAA CCA GCA GAG TC	CTG GAG TCA AGC CAG ACA CA
Foxa2	GCT CCC TAC GCC AAT ATC AA	CCG GTA GAA AGG GAA GAG GT
Foxg1	GAA CGG CAA GTA CGA GAA GC	TCA CGA AGC ACT TGT TGA GG
GDNF	CGC CCG CCG AAG ACC ACT CC	GTC GAA GGC GAC CGG CCT GC
GFAP	GCA GAC CTC ACA GAC GTT GCT	AGG CTG GTT TCT CGG ATC TGG
GLT1	ATC CTG GGA GCA GTA TGT GG	CTG ACA GCC CTG TGA TGA GA
GPC4	AGT GCC TTC AGT GCT CGA TT	CTT CCC GTT CCA ACA GTC AT
GPC6	AGC CAGATACCTGCCTGAGA	TCA TTG CCA TTG TAC GCA TT
GPX3	ACC AAT TTG GCA AAC AGG AG	AGC GGA TGT CAT GGA TCT TC
Hevin	ATT GGC AAC CAG AAG GAC AC	GGT TCT CAC TCT CGC CAG TC
IFN-α	GGT GGT GGT GAG CTA CTG GT	TTG AGC CTT CTG GAT CTG CT
IFN-β	CTG CCCTCTCCATCGACTAC	ACC CAG TGC TGG AGA AAT TG
IL-10	CCT GCT CTT ACT GGC TGG AG	TGT CCA GCT GGT CCT TCT TT
IL-12b	ACC CTC ACC TGT GAC AGT CC	TTC TTG TGG AGC AGC AGA TG
IL-13	ATC GAG GAG CTG AGC AAC AT	CGA GGC CTT TTG GTT ACA GA
IL-19	AGA AGG CAT GAA GGC ACA GT	TCA CGC AGC ACA CAT CTA CA
IL-1R2	CAT GGG AGA TGC AGG CTA TT	ACA CCT TGC ACG GGA CTA TC
IL-1RN	GAA AAG ACC CTG CAA GAT GC	GAT GCC CAA GAA CAC ATT CC

IL-1β	CTG TGA CTC GTG GGA TGA TG	GGG ATT TTG TCG TTG CTT GT
IL-2RA	CCA GAG AGT GAG GCT TCC TG	ACT CAG GAG GAG GAT GCT GA
IL-4	TCC TTA CGG CAA CAA GGA AC	GTG AGT TCA GAC CGC TGA CA
IL-6	ATG GAT GCT ACC AAA CTG GAT	TGA AGG ACT CTG GCT TTG TCT
iNOS	CAC CTT GGA GTT CAC CCA GT	ACC ACT CGT ACT TGG GAT GC
ITGαM	TTA CCG GAC TGT GTG GAC AA	AGT CTC CCA CCA CCA AAG TG
ITGβ4	GAA GGA ACT GCA GGT GAA GC	GCG ATG CGG ATA TCT CAT TT
Lmx1a	CCC CAA AAT CCG GAA TTA CT	CTCAGGGTCAGCAAAAGGAG
NF1A	ACC CGA GTA CCG AGA GGA TT	ACT GTG GGG ACT TCA CAA GG
NT3	GGT CAG AAT TCC AGC CGA TGA	GGC ACA CAC ACA GGA AGT GTC
Nurr1	ACC CTC TTC TGG ACA CAT GG	GCCATCACCACAAGACACAC
PAX6	AAC AAC CTG CCT ATG CAA CC	ACT TGG ACG GGA ACT GAC AC
Pitx3	CCA CCC TAC GAG GAG GTG TA	GGG CGG TGA GAA TAC AGG T
PRNP	GTG GCT ACA TGT TGG GGA GT	GTG AAG TTC TCC CCC TTG GT
S100β	GGC GGC AAA AGG TGA CCA GGA	GCC CTC ATG TCT GCC ACG GG
SERPIN B1B	ACC CGA GTA CCG AGA GGA TT	ACT GTG GGG ACT TCA CAA GG
SHH	AAA AGC TGA CCC CTT TAG CC	TGC ACC TCT GAG TCA TCA GC
SOD3	GAC CTG GAG ATC TGG ATG GA	GTG GTT GGA GGT GTT CTG CT
SPO1	TAC CAT GTC GGA GTG GAT CA	ACT CAC CCC ACT CAG TCA CC
SPO2	AGT GGA GCC AGA CAG CAT TT	CTC CTG CTG CTT CGA TCT CT
TGF-B	ATA CGC CTG AGT GGC TGT CT	TGG GAC TGA TCC CAT TGA TT
Thbs1	CCA GTT CAA CCA ACG TCC TT	TTG CGA ATG CTG TCC TGT AG
TNF-α	AGA TGT GGA ACT GGC AGA GG	CCC ATT TGG GAA CTT CTC CT
TXNIP	GGC ACA CTT ACC TTG CCA AT	ACT AGG GGC AGA TCG AGG AT
Vimentin	AGA TCG ATG TGG ACG TTT CC	CAC ACT GTC TCC GGT ATT CGT
Wnt1	CTT CGG CAA GAT CGT CAA CC	GCG AAG ATG AAC GCT GTT TCT
Wnt3a	GAA CGC GAC CTG GTC TAC TAC G	GTT AGG TTC GCA GAA GTT GGG T
Wnt4	GCC ACG CAC TAA AGG AGA AG	GGC CTT AGA CGT CTT GTT CG
Wnt5a	AAT AAC CCT GTT CAG ATG TCA	TAC TGC ATG TGG TCC TGA TA
Wnt7a	CGA GAG CTA GGC TAC GTG CT	CTG AGG GGC TGT CTT ATT GC
YM1	TCG TGA GAA GCT CAT TGT GG	AAC CCA TAC ATT GCC CTG AA

Supplementary Table 2. Primary antibodies used in this study.

Antibodies	Working dilution	Company	Catalog number
Mouse monoclonal Antibody(Ab)			
Bassoon	1:400	[6]Enzo life science	ADI-VAM-PS003-D
CD16/32	1:500	[2]BD Biosciences	553142
CD44	1:500	[11]Novus Biologicals	.NBP1-31488
Gephyrin	1:500	[16]Synaptic Systems	147 011
GFAP	1:200	[8]MP Biomedicals	691102
GLAST	1:1000	[9]Miltenyi Biotec	130-095-821
HuC/D	1:100	[7]Chemicon	A21271
iNOS	1:1000	[2]BD Biosciences	610432
NeuN	1:200	[10]Millipore	MAB377
Nurr1	1:1000	[13]R&D Systems	PP-N1404-00
Synapsin 1	1:1000	[2]BD Biosciences	611392
SV2	1:50	[5]DHSB	2315387
Synaptophysin	1:1000	[2]BD Biosciences	611880
Tyrosine Hydroxylase (TH)	1:200	[7]Immunostar	T-1299
Rabbit polyclonal Ab			
CD206	1:500	[1]Abcam	ab64693
GFAP	1:400	[4]DAKO	Z0334
GLT-1	1:200	[1]Abcam	ab106289
Iba-1	1:200	[15]Wako	019-19741
Lmx1a	1:2000	[10]Millipore	AB10533
Nurr1	1:500	[14]Santa Cruz	sc-991
TH	1:1000	[12]Pel-freez	P40101
S100β	1:500	[1]Abcam	ab868
Sox2	1:100	[3]Chemicon	AB5603
vGAT	1:1000	[16]Synaptic Systems	131 003
vGLUT2	1:1000	[16]Synaptic Systems	135 403
Goat polyclonal Ab			
Arg1	1:500	[11]Novus Biologicals	NB100-59740
Foxa2	1:500	[14]Santa Cruz	sc-6554
PSD95	1:500	[16]Synaptic Systems	124 014
Rat polyclonal Ab			
CD11B	1:500	[10]Millipore	CBL1512
Chicken polyclonal Ab			
Tyrosine Hydroxylase (TH)	1:500	[1]Abcam	ab76442

1. Abcam, Cambridge, MA, UK
2. BD Biosciences, Franklin Lakes, NJ, USA
3. Chemicon, Temecula, CA, USA
4. DAKO, Carpinteria, CA, USA
5. DSHB, U. Iowa, Iowa City, IA
6. Enzo life science, Farmingdale, NY, USA
7. Immunostar, Hudson, WI, USA
8. MP Biomedicals, Santa Ana, CA, USA
9. Miltenyi Biotec, Bergisch Gladbach, Germany
10. Millipore, Pittsburgh, PA, USA
11. Novus Biologicals, Littleton, Colorado, USA
12. Pel-Freez, Rogers, AR, USA
13. R&D Systems, Minneapolis, MN, USA
14. Santa Cruz Biotechnology, Santa Cruz, CA, USA
15. Wako, Osaka, Japan
16. Synaptic systems, Göttingen, Germany

Supplementary references

1. Tom, V.J., Steinmetz, M.P., Miller, J.H., Doller, C.M., and Silver, J. 2004. Studies on the development and behavior of the dystrophic growth cone, the hallmark of regeneration failure, in an in vitro model of the glial scar and after spinal cord injury. *J Neurosci* 24:6531-6539.
2. Dobin, A., Davis, C.A., Schlesinger, F., Drenkow, J., Zaleski, C., Jha, S., Batut, P., Chaisson, M., and Gingeras, T.R. 2013. STAR: ultrafast universal RNA-seq aligner. *Bioinformatics* 29:15-21.
3. Bolstad, B.M., Irizarry, R.A., Astrand, M., and Speed, T.P. 2003. A comparison of normalization methods for high density oligonucleotide array data based on variance and bias. *Bioinformatics* 19:185-193.